Research, Society and Development, v. 11, n. 8, e2211830629, 2022
(CC BY 4.0) | ISSN 2525-3409 | DOI: http://dx.doi.org/10.33448/rsd-v11i8.30629

Characterization of Ti-6Al-4V titanium alloy applied in hydroxyapatite coated hip prostheses

Caracterização da liga de titânio Ti-6Al-4V aplicada em próteses de quadril revestidas com hidroxiapatita

Caracterización de la aleación de titanio Ti-6Al-4V aplicada a prótesis de cadera recubiertas de hidroxiapatita

Received: 05/20/2022 | Reviewed: 06/02/2022 | Accept: 06/03/2022 | Published: 06/07/2022

Caique Movio Pereira de Souza
ORCID: https://orcid.org/0000-0002-3741-1036
Mackenzie Presbiterian University, Brazil
E-mail: caiquemovio@gmail.com
Vanderlei Araujo Militão
ORCID: https://orcid.org/0000-0002-3775-3896
National Service for Industrial Apprenticeship, Brazil
E-mail: vamilitao@terra.com.br
Isaias Gouveia Silva
ORCID: https://orcid.org/0000-0002-0789-3089
National Service for Industrial Apprenticeship, Brazil
E-mail: isaias.gouveia@sp.senai.br
Rene Ramos de Oliveira
ORCID: https://orcid.org/0000-0002-7131-204X
Institute of Energy and Nuclear Research, Brazil
E-mail: roliver1969@gmai.com
Vanessa Seriacopi
ORCID: https://orcid.org/0000-0002-1903-867X
Maua Institute of Technology, Brazil
E-mail: vanessa.seriacopi@gmail.com
Wilson Carlos da Silva Junior
ORCID: https://orcid.org/0000-0001-8128-281X
Federal Institute of Education, Science, and Technology of São Paulo, Brazil
E-mail: wilsoncarlos@ifsp.edu.br

Abstract
Titanium and its alloys are widely used as biomaterials in hard tissue replacements due to their unique physiological environment responses and chemical and mechanical properties, such as corrosion resistance, fatigue resistance, and ductility. Other metals used as biomaterials have elastic modulus with values ten times higher than human bone, which can cause failure when there are impacts. Several studies report hip prosthesis failures due to fatigue. This article aims to carry out studies on the mechanical properties and fatigue resistance in an environment that simulates those of the joints of the human body, using hip prostheses manufactured with Ti 6Al 4V alloy with hydroxyapatite coating. Samples were taken from the neck region for microstructural characterization to identify grain size, inclusions, microhardness, tensile test, scanning electron microscopy, energy dispersion spectroscopy, X-ray fluorescence,e, and X-ray diffraction also performed. After applying more than 10,000,000 cycles with compressive forces ranging from -0.3 kN to -3.0 kN, no cracks were found and it was observed that the part suffered only elastic deformations.
Keywords: Hip prosthesis; ASTM F136; Fatigue Tests.

Resumo
O titânio e suas ligas são amplamente utilizados como biomateriais em substituições de tecidos duros devido a sua resposta única em contato com o ambiente fisiológico e as suas propriedades químicas e mecânicas, como resistência à corrosão, resistência à fadiga e ductilidade. Outros metais utilizados como biomateriais possuem módulo de elasticidade com valores dez vezes maiores que o osso humano, o que pode causar falhas quando há impactos. Vários estudos relatam falhas de próteses de quadril devido à fadiga. Este artigo tem como objetivo realizar estudos sobre as propriedades mecânica e resistência à fadiga em um ambiente que simule as articulações do corpo humano, utilizando próteses de quadril fabricadas com liga Ti 6Al 4V com revestimento de hidroxiapatita. As amostras foram retiradas da região do pescoço para caracterização microestrutural para identificação do tamanho de grão, inclusões, microdureza,

ensaio de tração, microscopia eletrônica de varredura, espectroscopia de dispersão de energia, fluorescência de raios X e difração de raios X. Após a aplicação de mais de 10.000.000 ciclos com forças de compressão variando de -0,3 kN a -3,0 kN, não foram encontradas trincas e observou-se que a amostras sofreram apenas deformações elásticas.
Palavras-chave: Prótese de quadril; ASTM F136; Ensaio de Fadiga.

Resumen
El titanio y sus aleaciones se utilizan ampliamente como biomateriales en reemplazos de tejidos duros debido a sus respuestas ambientales fisiológicas únicas y sus propiedades químicas y mecánicas, como la resistencia a la corrosión, la resistencia a la fatiga y la ductilidad. Otros metales utilizados como biomateriales tienen módulos elásticos con valores diez veces superiores al hueso humano, lo que puede causar fallas cuando hay impactos. Varios estudios reportan fallas de prótesis de cadera debido a la fatiga. Este artículo tiene como objetivo realizar estudios sobre las propiedades mecánicas y la resistencia a la fatiga en un ambiente que simula las articulaciones del cuerpo humano, utilizando prótesis de cadera fabricadas con aleación Ti 6Al 4V con recubrimiento de hidroxiapatita. Se tomaron muestras de la región del cuello para caracterización microestructural para identificar tamaño de grano, inclusiones, microdureza, prueba de tracción, microscopía electrónica de barrido, espectroscopía de dispersión de energía, fluorescencia de rayos X, y también se realizó difracción de rayos X. Después de aplicar más de 10.000.000 de ciclos con fuerzas de compresión en el rango de -0,3 kN a -3,0 kN, no se encontraron grietas y se observó que la pieza solo sufría deformaciones elásticas.
Palabras clave: Prótesis de cadera; ASTM F136; Pruebas de fatiga.

1. Introduction

For centuries, efforts have focused on developing components to effectively repair or replace damaged parts of human tissue. Catheters, stents, plates, pins, lenses, prostheses, and countless other implanted devices enabled survival and restored the functionality of biological systems, improving quality of life (Antonelli, 2011). The development of new metal alloys for application in biomaterials and advanced surgical techniques have improved the quality of life of millions of people who had dysfunctions where these metals replaced members of the human body (Souza,2022).

The main causes of failure of an orthopedic metallic biomaterial, such as those used in hip prostheses, are commonly related to the failure to meet the properties necessary for its good performance, which include resistance to fatigue, which can fail the Prosthesis, and even strains (Wang,2013). Cyclic changes are caused by the movement of the human gait, which can result in fracture due to fatigue, or lead to implant loosening (Nassab, 2010).

Fatigue fractures occur due to the actions of stress concentrating agents in certain geometric locations (Chen, 2015). The site that suffers the greatest tension applied to the stem is the neck region of the hip prosthesis, where approximately 200 to 350 MPa is applied (Liu, 2019). The fatigue limit of implantable alloys depends on factors such as the manufacturing process, surface conditions, microstructure, and stress application conditions, which are related to the movements of individuals (Silva Junior, 2021).

Titanium alloys have been used as implant materials because of their desirable characteristics, such as low density (compared to stainless steel), high corrosion resistance, biocompatibility, and excellent mechanical properties. Titanium and its alloys stand out among the main metallic alloys used in implants, mainly Ti-6Al-4V, because of its high strength-to-weight ratio, mechanical properties at high temperatures, and high corrosion resistance. Approx. 50% of the titanium alloys produced in the world are Ti-6Al-4V (Rocha, 2018).

Commercially pure titanium consists, at room temperature, of a single-phase, with a hexagonal close-packed (HC) crystal structure, called the α-phase. Titanium exhibits an allotropic transformation upon reaching 882 °C (critical temperature). At temperatures above the critical temperature, commercially pure titanium consists of a single phase, with a body-centered cubic (BCC) structure, called the β phase (Couto,2006). The addition of alloying elements can stabilize the α or β phases, so titanium alloys can present, at room temperature, a single α structure, a single β structure, or a mixture of these two phases (α + β alloys). Aluminum is an α-stabilizer, and vanadium is a β-phase stabilizer, which is why Ti-6Al-4V is classified as an α+β alloy (Kirchner, 2015).

The addition of aluminum and vanadium to the titanium alloy also causes a change in fatigue strength, yield strength, hardness, microstructure, fracture pattern, and elongation, but the modulus of elasticity is almost unchanged compared to titanium pure (Costa,2009). The Ti-6Al-4V alloy has twice the value of tensile strength compared to pure titanium, maintaining the low density that provides a reduction in the weight of the prosthesis, thus increasing the comfort of the user, for having a prosthesis of smaller size (Brandla, 2011).

Hydroxyapatite (HA) has been widely studied in recent decades due to its physicochemical properties suitable for bone tissue repair, which constitute from 30% to 70% of the mass of bones and teeth, favoring osteoconductivity, enabling the bone growth in the places where it is found, it has bioactivity not producing immunological or inflammatory reactions, in addition to facilitating the proliferation of bone cells, being therefore suitable for orthopedic and dental implants (Sidane,2015).

Bone formation in implants is significantly greater over coated implants than in uncoated titanium implants (Rafi, 2013). Although walking is an unconscious and almost automatic movement, it is highly complex, as it requires the perfect harmony of the body internally, opposing the external forces that are in constant action on the segments and joints (Souza,2022).

The interest in studying internal forces and movements is linked to the relationship between internal forces developed in the body and the development of injuries in the musculoskeletal system (Bahrm, 2005). From the directions and magnitudes of the static and cyclic forces that occur in the joints, it is possible to assess the possibilities of injuries during the performance of different movements and positions (Cantergi,2011). Gait alteration is a frequent problem with aging. During gait, the efforts acting on the joints can vary from zero to seven times the body weight (Paul,1976). It is estimated that the peak contact stress at the hip can reach 20 MPa during stair climbing (Hodge,1986).

Orthopedic implants are subjected to static and/or dynamic efforts, most of the time of relevant magnitudes, so it is necessary to verify the durability and what are the possible failures that can happen in hip, knee, and shoulder prostheses, through the performance of the fatigue test meeting the new requirements of ANVISA (National Health Surveillance Agency), which changed the minimum number of cycles from 5,000,000 to 10,000,000 to be supported without failure by hip prostheses.

2. Methodology

For the realization of this article, specimens of Ti-6Al-4V alloy were used, three taken from a cylindrical bar with the dimensions of 15 x 150 mm², from which hip prostheses are manufactured and three of hip prostheses with coating, from which other specimens were taken for analysis. The samples were subjected to several tests shown in the flowchart in Figure 1.

Figure 1: Sample embedded a) cylindrical sample and b) sample is taken from the neck of the prosthesis.

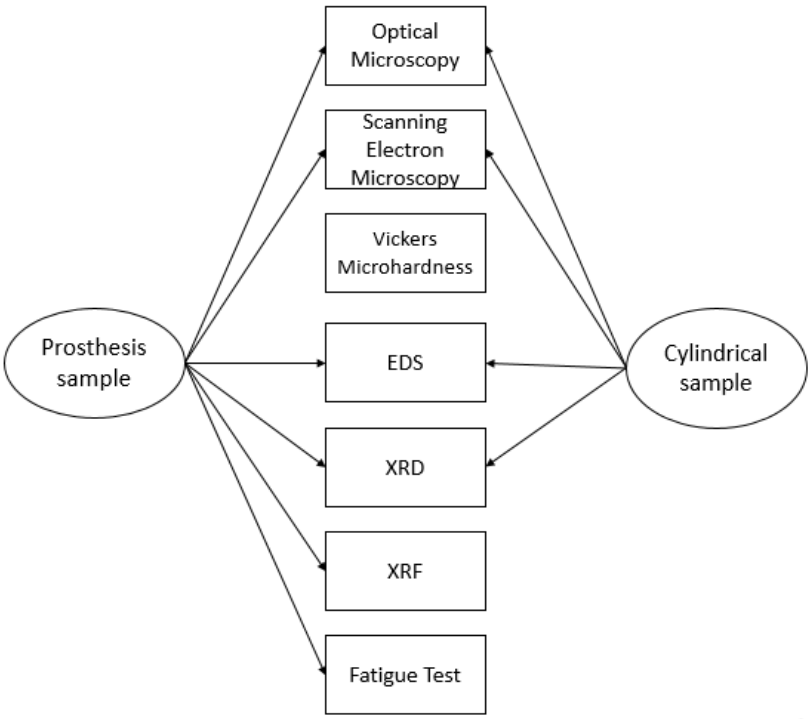

Source: Authors.

Figure 2 shows two samples being a) taken from a billet of the Ti6Al4V alloy that was received as raw material for the production of prostheses and b) a sample from the neck region of the prosthesis after the fatigue testing of metallographic preparation using conventional techniques such as embedding, sanding, polishing and chemical etching following the instructions of the ASTM E3 standard.

Figure 2: Embedded sample a) cylindrical sample and b) sample taken is taken the neck of the prosthesis.

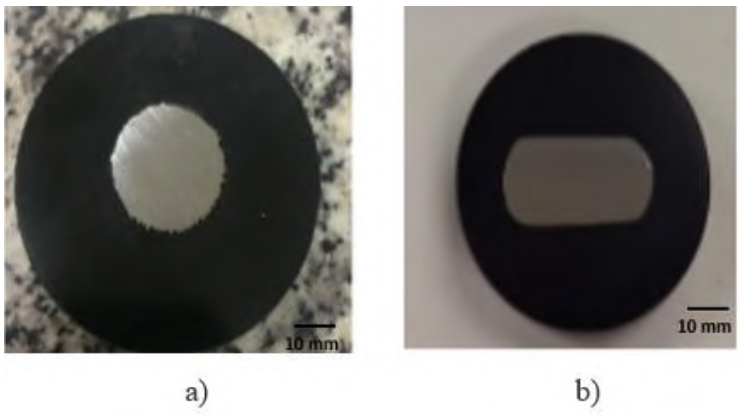

Source: Authors.

In the observation of the samples, an optical microscope Olympus BX60M was used coupled with an iman age scanning and analysis system. In addition, a Jeol scanning electron microscope, model JSM-6010LA, coupled to a chemical

analysis system using energy dispersion-EDS spectroscopy was used. In the Vickers (HV) microhardness test, a Buehler 1600 microhardness tester with a diamond indenter was used with an application of 500 gf.

The inclusion content was determined according to the ABNT NBR NM 88:1996 standard, following method 1 presented in the standard. For each image observed, inclusions from levels 1 to 5 were recorded, for each fine or coarse series and, in the end, the average of the highest density values recorded in the sample was calculated. With the average of these values, at the end of the analysis of the specimen, the content of inclusions, for each series, of the analyzed material was indicated. X-ray diffraction tests were performed in a Malvern PanAlytical Empyrean equipment, and a generator tube with Cu anode, with a voltage of 45 kV and 40 mA, with a 2θ variation from 10° to 110°, the step of 0.02° and with a step time of 3s. For the determination of the chemical elements present in the sample, a semiquantitative analysis was carried out, by the analytical technique of X-ray fluorescence (FRX) by energy dispersion, the method used for analysis was the direct one, the Ti6Al4V sample was positioned in a sample holder micro X-cell-SPEX, performed on a Shimadzu EDK-720 equipment. For the fatigue test, support was developed for positioning the prosthesis at the angle required by the test standard (put the standard number), as shown in Figure 3.

Figure 3: Prosthesis positioned through the support.

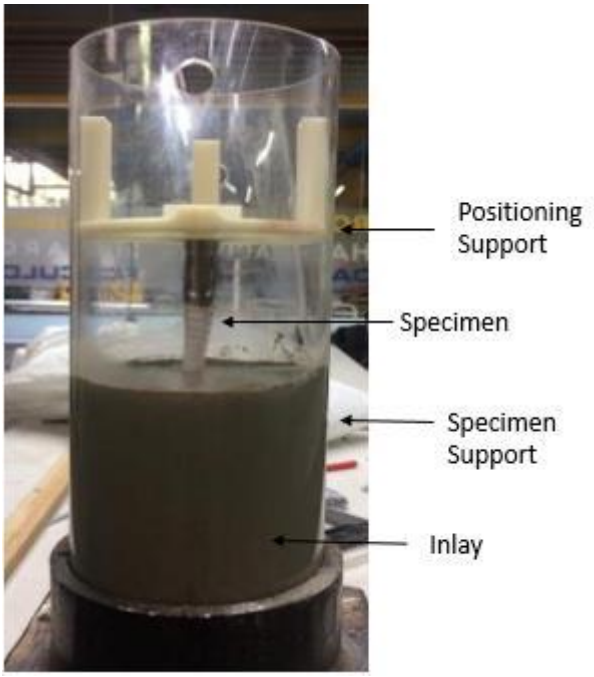

Source: Authors.

For the fatigue test, a device for positioning the prosthesis was built. Complying with the ABNT NBR ISO 7206-4 standard indicates the correct load application point, which may imply an error in the analysis of the performance of the prostheses in case of application at another point. Figure 4a shows the device built as a template and which positions the prosthesis so that its point of application is as indicated by the standard, where the values of angles α equal to 10° and β equal to 9°, that is, there is a guarantee that the forces were applied correctly.

Figure 4: Fatigue test device: a) constructed device, b) test preparation.

Source: Authors.

For test bodies (CT) that are 200 mm long, it is necessary to place 80 mm of the prosthesis embedded in cement, the alpha angle will be 10° and the beta angle will be 9°. After positioning the prosthesis in the cement and resting for 24 hours to obtain maximum strength, the fatigue test was performed on an Instron 8801 machine, with the parameters adjusted for a compressive load, with a frequency of 15 Hz with a load of maximum -0.3 kN and minimum -3.0 kN, the fatigue test followed the ABNT NBR 7206-4 standard, Figure 4b. The tensile test was carried out in EMIC equipment, model DL20000, following the ABNT NBR ISO 6892-1:2013 standard – Metallic materials - Tensile Test. The samples were subjected to tensile force until the material rupture to determine mechanical properties (elongation, deformation, and tensile strength, among other parameters).

3. Results and Discussion

Figure 5 shows a micrograph of the Ti6Al4V alloy of the cylindrical sample. It is possible to observe the presence of the α phase and the β phase. It is possible to notice a homogeneity in the structure, the desired characteristic in orthopedic implants as its results, resulting in animal properties in service, such as fatigue resistance.

Figure 5: Microstructure of the titanium alloy Ti-6Al-4V of the cylindrical sample at 1000x magnification.

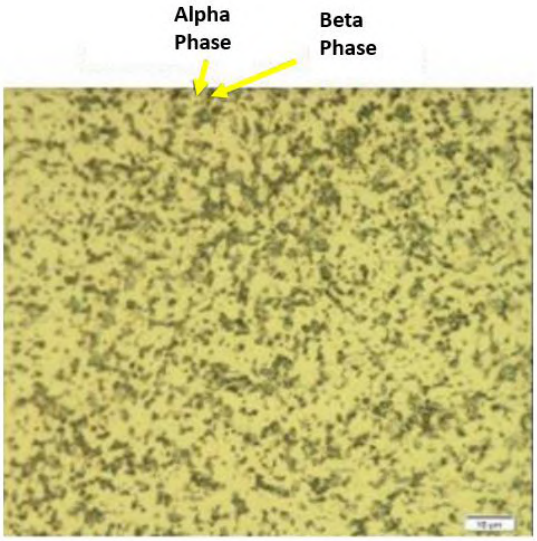

Source: Authors.

The microstructure of the sample taken from the neck region of the prosthesis is shown in Figure 6, it is observed that the grains of the alpha phase had an increase in size after the fatigue test, caused by the deformation suffered by the prosthesis.

Figure 6: Microstructure of the titanium alloy Ti-6Al-4V of the prosthesis at 1000x magnification.

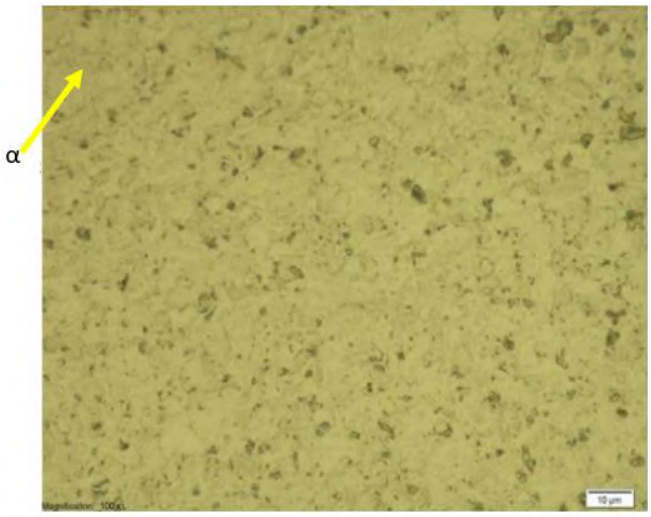

Source: Authors.

The grain size was calculated using the ImageJ software and the Heyn intercept method, shown in Figure 7, in the result obtained with ImageJ, the average grain diameter was 4.94 nm and the average grain area was 31, 16 μm², in the Heyn intercept method, the value of 4.88 nm in mean grain diameter. In this way the two results obtained correspond to ABNT (TG) grain size number 12, thus corresponding to ABNT NBR 11568:2016 grain size number 5 or finer.

$$I = \frac{C}{A.N} = \frac{132\mu m}{27.1000} = 4{,}88 \text{ n}$$

Figure 7: Microstructure used in the Heyn intercept method.

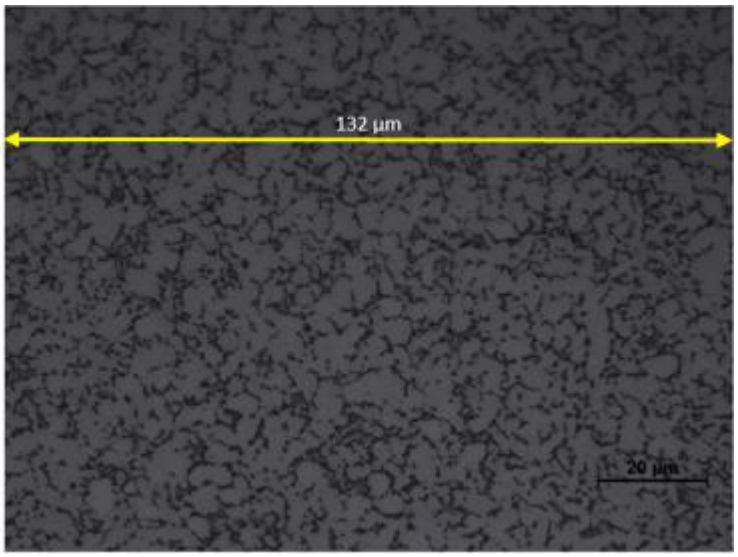

Source: Authors.

The results of Vickers microhardness can be seen in Table 1, the values obtained showed no deviation considered, showing homogeneity of the structure of the titanium alloy. Based on the literature [14], the estimated value for the Vickers microhardness of the Ti-6Al-4V alloy is 349 HV, in the test performed the values found were as follows:

Table 1: Vickers Microhardness result.

Indentations	$HV_{0,500}$
1	362,1
2	358,5
3	342,8
4	342,8
5	342,1
6	344,2
7	343,5
8	333,8
9	348,9
10	365,0
Average	348,37
Standard deviation	10,12
Amplitude	31,2

Source: Authors.

The analysis of the samples' inclusions content revealed the presence of inclusions of type A and B, respectively sulfides and aluminates, and only inclusions of type C and D, called silicates and globular oxides, respectively, in type C inclusions were not detected. severity 1 was not reached, and in type D severity 1.5 was not reached, both in the fine series and in the coarse series. Another point that can be analyzed in Figure 8 is the presence of OS (silicate-type oxides) and globular oxides (GO). The observation by meausingal microscopy of the Ti-6Al-4V alloy revealed the presence of a small amount number of spots, identified as inclusions and porosities, but which could not be differentiated at this magnification, the analyzed images can be seen in Figure 8.

Figure 8: Determination of inclusions content: a) 100x magnification, b) 500x magnification.

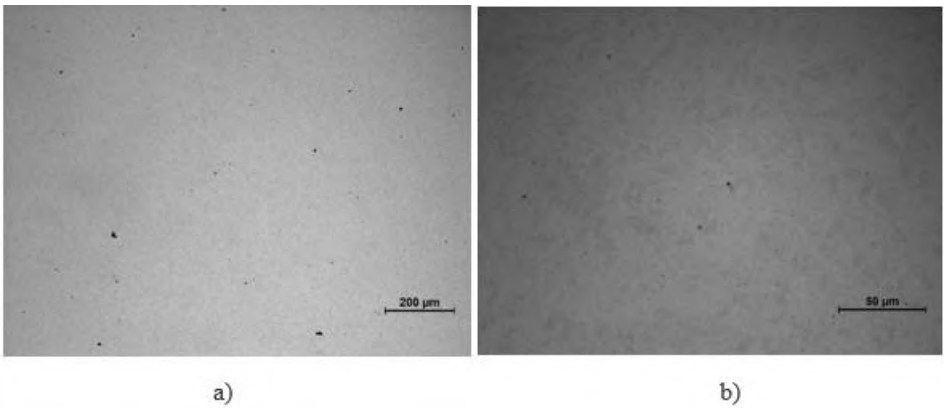

Source: Authors.

In Figures 9 and 10, the presence of two phases α (compact hexagonal) and β (body-centered cubic) can be noted in the micrograph. Thus, it can be affirmed that this alloy is α+β, and the β phase is homogeneously distributed in the α matrix.

Figure 9: Microstructure of the cylindrical sample with 1000x magnification – SEM – Secondary electrons.

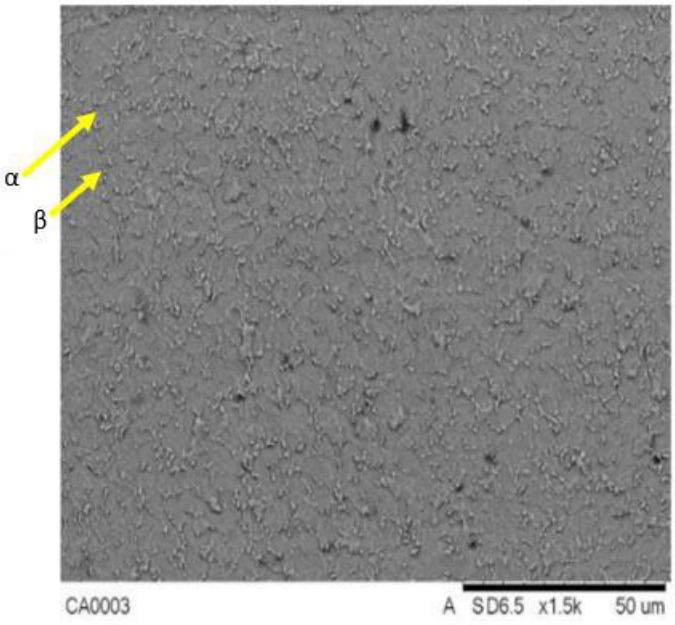

Source: Authors.

Figure 10: Microstructure of the cylindrical sample with 3000x magnification – SEM – Secondary electrons.

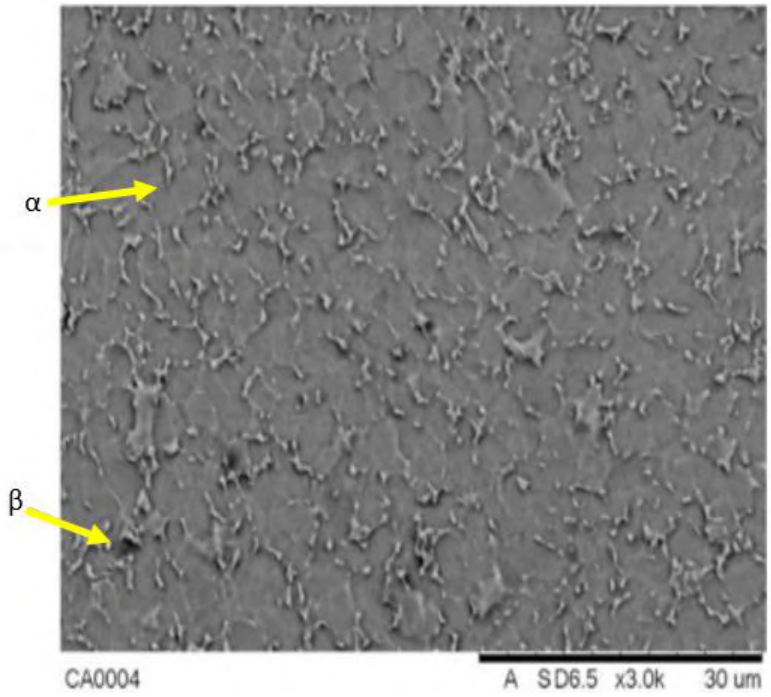

Source: Authors.

Figure 11 shows the presence of a substructure inside the grains composed of lamellar phases α and β. This substructure is formed by lamellae of the α phase inside originally β grains. The β phase is predominant in the subgrain contours. It is also possible to notice the formation of a lamellar microstructure, in extremely final shapes, resembling needles, characteristic of the alpha phase.

Figure 11: Microstructure of samples after fatigue test with 1500x magnification. – SEM – Secondary electrons.

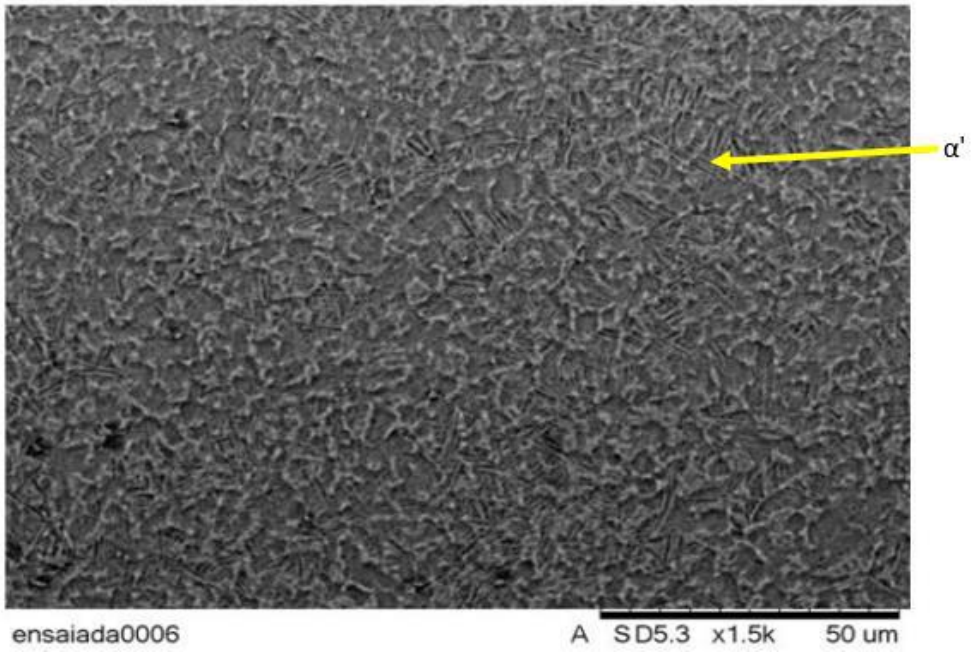

Source: Authors.

The change in the microstructure is due to the mechanical work caused by the fatigue test. This change in the microstructure will also occur during the use of the user since, in a normal walk, a force of 7.6 times the user's weight can be applied (Nassab,2010).

In order the presence of α and β phases in the samples, analyzes were performed with X-Ray Diffraction (XRD). Figure 12 shows the diffractogram obtained in the XRD analysis of the cylindrical sample and of the prosthesis tested, where the points of greatest mechanical stress were selected, compared with the JCPDS database, using the Crystallographica-Search Match program.

Figure 12: X-ray Diffraction of Ti-6Al-4V sample.

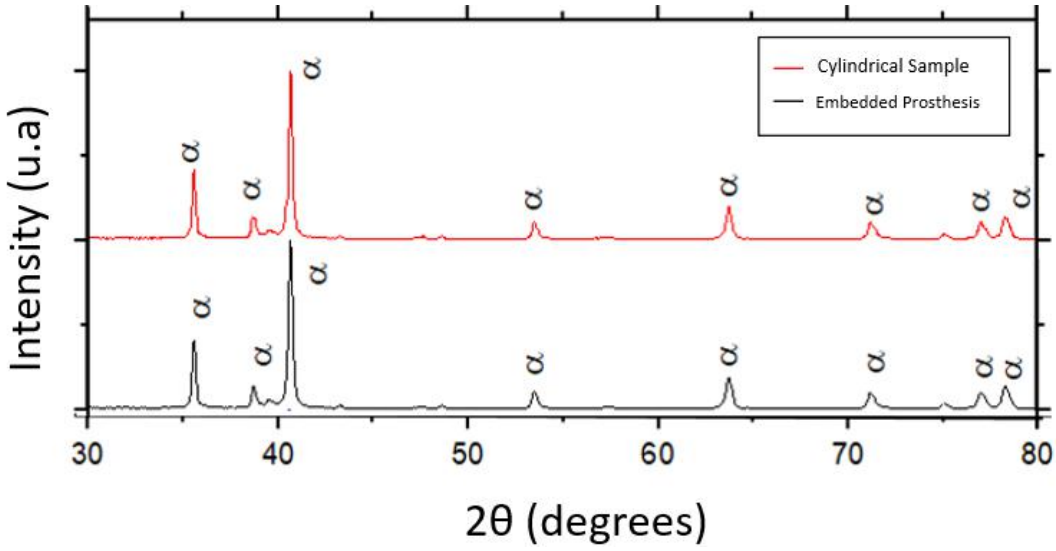

Source: Authors.

Based on the XRD results, it was possible to notice a difficulty in identifying the β phase in titanium alloys when the α phase is also present. This occurs because the most intense reflection plane of phase β (110) has a position coincident with a reflection plane of phase α (002) so that the result is masked. As the percentage of β phase in the Ti-6Al-4V alloy is relatively low and the other non-coincident reflections are of low intensity, it is practically impossible to ensure the presence of the β phase only.

For a more complete analysis of the phases and elements present, energy dispersive spectroscopy (EDS) was performed ed, as shown in Figure 13, which showed the presence of nitrogen, vanadium, iron, and aluminum.

Figure 13: Energy Dispersive Spectrum (EDS) of the cylindrical sample.

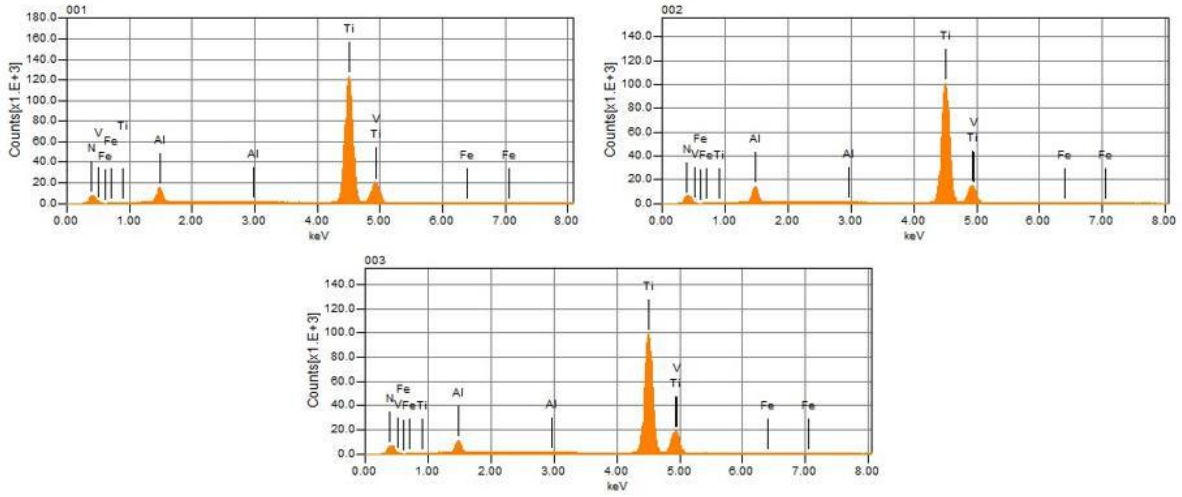

Source: Authors.

Figure 14 shows the diffractograms of the sample taken from the prosthesis, titanium peaks, and the presence of aluminum, carbon, and oxygen. In this way, the possibility of any type of contaminant in the samples is excluded.

Figure 14: Energy Dispersive Spectrum (EDS) of the neck of the prosthesis.

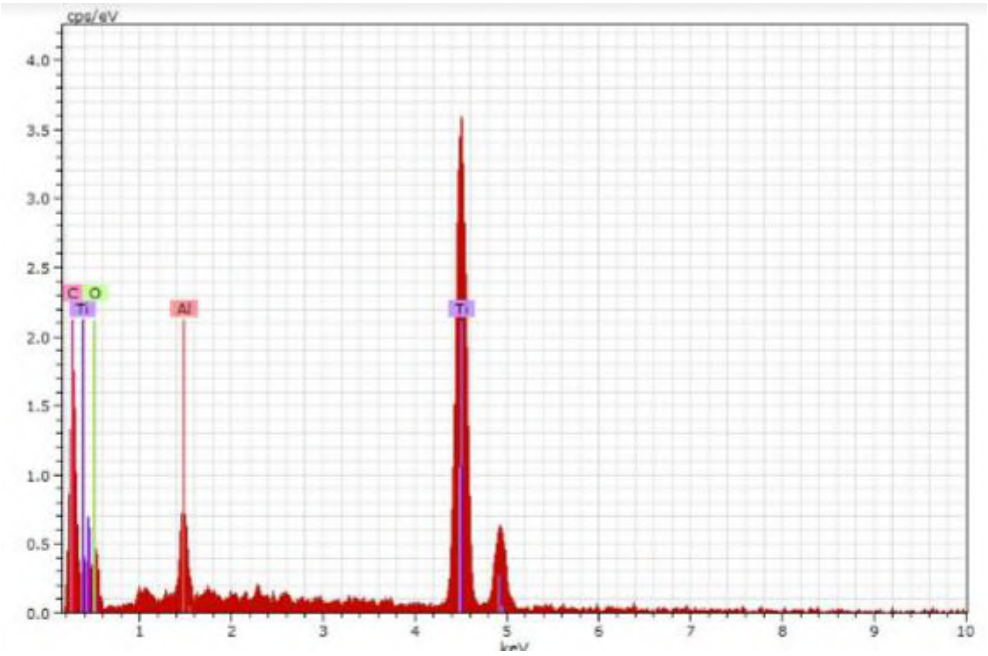

Source: Authors.

Because the dispersion energy of titanium and vanadium are close, it was not possible to obtain an exact result of the presence of vanadium in the sample. Material has the presence of titanium, aluminum, vanadium, and iron, as can be seen in Table 2.

Table 2: X-ray fluorescence result.

Maximum Composition (%) p/p		Sample Values (%)
Oxygen	0,20	0
Carbon	0,10	0
Iron	0,20	0,203
Aluminum	5,5-6,75	5,3
Vanadium	3,5-4,5	4,1

Source: Authors.

In the fatigue test with a frequency of 15Hz, the prostheses were subjected to cycles with loads between -0.3KN and -3.0 kN, showing no deformity, fracture, or oxidation, the test lasted 8 days and presented similar results in the three trials. The prosthesis was subjected to a visual inspection to check for non-conformities and possible cracks after the fatigue test to which it was submitted. In Figure 15a it is possible to verify the deformation of the prosthesis in the cycle to which it was submitted, according to the sampling of 1 million cycles. The deformation of the prosthesis remained at 0.3 mm steadily, as shown in Figure 15b.

Figure 15: Behavior of the prosthesis at the beginning and end of the fatigue test.

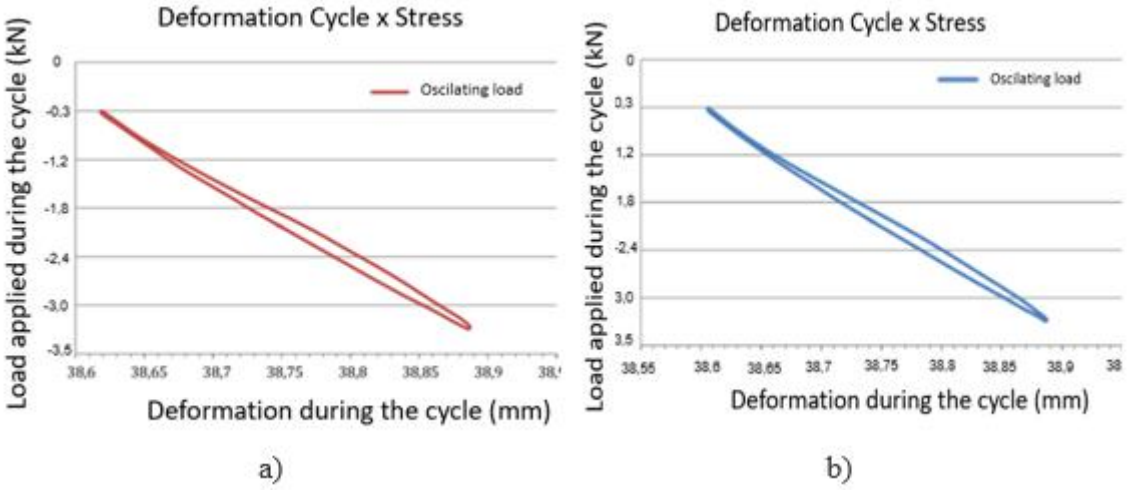

Source: Authors.

The tensile test was evaluated following the standards of ABNT NBR ISO 6892-1:2013. The standard establishes 897 MPa as the minimum value of the tensile strength limit. In Figure 16, it is possible to verify the stress versus deformation graphs of the specimens, three tensile specimens of the Ti-6Al-4V alloy were tested.

Figure 16: Stress x Deformation Chart: a) specimen 1 , b) specimen 2 and c) specimen 3

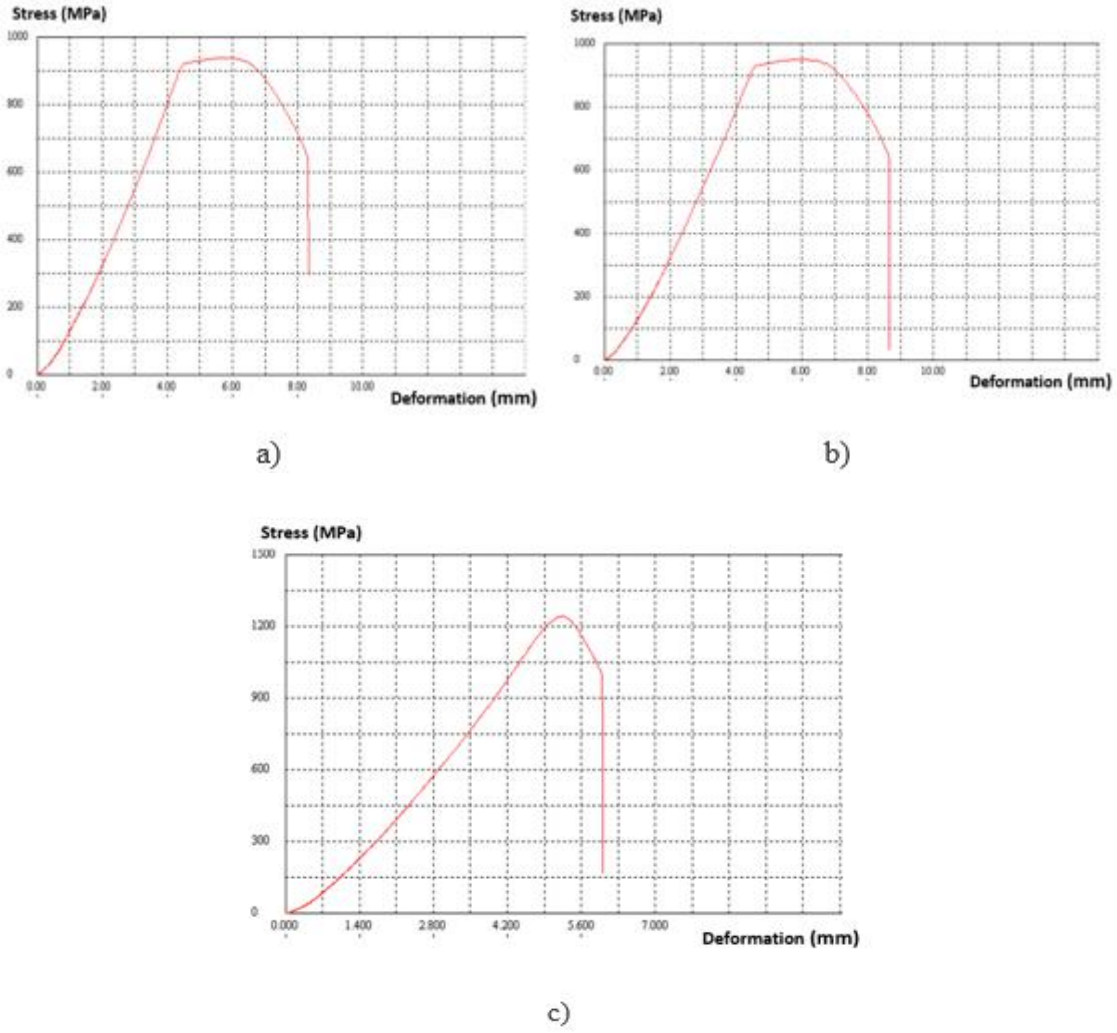

Source: Authors.

The results provided by the tensile test equipment for the specimens are presented in Table 3. The results presented meet the minimum indicators of the ASTM F138 standard, thus the mechanical behavior presented is within the values expected by the literature.

Table 3: Tensile test result.

Body of Test	Specimen área (mm)	Flow Limit (MPa)	Tensile Strength Limite (MPa)
1	28,274	920	956,82
2	28,274	935	969,16
3	28,274	1266,1	1266,10
Average	28,274	1040,36	1064,02

Source: Authors.

According to data obtained in the tensile test, it was possible to notice that the specimens presented adequate mechanical strength results. Following the ASTM F136 standard, where a yield strength of 828 MPa is recommended, and the yield strength stress is the recommended parameter for use in projects, the results obtained show that the specimens studied are within the minimum required for use in implants.

4. Conclusion

The inclusions are within the standards required by the ABTN NBR NM 88:1996 standard, the grain size obtained was 4.94 nm by the Image J software and the Heyn method 4.88 nm, which corresponds to ABNT (TG) nº12 which complies with the ABNT 11568:2016 standard, which meets the manufacturing standards for surgical implants. The chemical composition obtained by EDS and FRX, shows the contents of the elements present within the regulations. Microscopy shows the balanced presence of the alpha and beta phases before and after the deformations suffered by the tested prostheses. In the X-Ray diffraction patterns in the sample peaks were perceptible, evidencing the identification of the α and β phases, being able to affirm that the Ti-6Al-4V alloy is an α+β mixture, and β is distributed homogeneously in the α matrix, finding the components the vanadium carbonates. The fatigue test of the prosthesis provided evidence that the component withstood more than 10,000,000 without failures or cracks, it appears that the prostheses suffered only elastic deformation. The mechanical properties obtained in the tensile test exceed the minimum values required by the standard, the tensile strength limit found 1064 MPa being within the minimum required for use in implants. The Vickers microhardness found was 348.37 HV0.500.

Acknowledgments

The authors are very grateful to CNPq (National Council for Scientific and Technological Development), for the scholarship and financial assistance, which allow full dedication to the Universidade Presbiteriana Mackenzie graduate program and operationalization of the study.

References

Antonialli, A. Í. S., & Bolfarini, C. (2011). Numerical evaluation of reduction of stress shielding in laser coated hip prostheses. *Materials Research*, 14(3),331 334. https://doi.org/10.1590/s1516-14392011005000043

Bahr, R., & Krosshaug, T. (2005). Understanding injury mechanisms: a key component of preventing injuries in sport. *British Journal of Sports Medicine*, 39(6), 324–329. https://doi.org/10.1136/bjsm.2005.018341

Brandl, E., Leyens, C., & Palm, F. (2011). Mechanical Properties of Additive Manufactured Ti-6Al-4V Using Wire and Powder Based Processes. IOP *Conference Series: Materials Science and Engineering*, 26, 012004. https://doi.org/10.1088/1757-899x/26/1/012004

Cantergi, D. (2011). Avaliação das forças musculares envolvidas no exercício de extensão do quadril e joelho do método Pilates [Dissertação].

Chen, Q., & Thouas, G. A. (2015). Metallic implant biomaterials. Materials Science and Engineering: *R: Reports*, 87, 1–57. https://doi.org/10.1016/j.mser.2014.10.001

Costa, A. C. M. F., Lima, G. M., Lima, H. M. A., Cordeiro, V. V., Viana, K. M. S., & Souza, C. V. (2009). Hidroxiapatita: Obtenção, caracterização e aplicação. *Revista Eletrônica de Materiais e Processos*. http://www2.ufcg.edu.br/revista-remap/index.php/REMAP/article/view/105

Couto, A. A., Faldini, S. B., Almeida, G. F. C., Sekeres, T. S., Kunioshi, C. T., Morcelli, A. E., & Lima, N. B. (2006). Caracterização microestrutural da liga Ti-6Al-4V comercial utilizada como biomaterial.

Hodge, W. A., Fijan, R. S., Carlson, K. L., Burgess, R. G., Harris, W. H., & Mann, R. W. (1986). Contact pressures in the human hip joint measured in vivo. *Proceedings of the National Academy of Sciences*, 83(9), 2879–2883. https://doi.org/10.1073/pnas.83.9.2879

Kirchner, A., Klöden, B., Luft, J., Weißgärber, T., & Kieback, B. (2015). Process window for electron beam melting of Ti-6Al-4V. *Powder Metallurgy*, 58(4), 246–249. https://doi.org/10.1179/0032589915z.000000000244

Liu, S., & Shin, Y. C. (2019). Additive manufacturing of Ti6Al4V alloy: A review. *Materials & Design*, 164, 107552. https://doi.org/10.1016/j.matdes.2018.107552

Nasab, M. B., & Hassan, M. R. (2010). Metallic biomaterials of knee and hip--a review. 24 (2), 69-82. https://link.gale.com/apps/doc/A308129449/HRCA?u=googlescholar&sid=googleScholar&xid=3b4d2143

Paul, J. P. (1976). Approaches to design - Force actions transmitted by joints in the human body. Proceedings of the Royal Society of London. Series B. *Biological Sciences*, 192(1107), 163–172. https://doi.org/10.1098/rspb.1976.0004

Rafi, H. K., Karthik, N. V., Gong, H., Starr, T. L., & Stucker, B. E. (2013). Microstructures and Mechanical Properties of Ti6Al4V Parts Fabricated by Selective Laser Melting and Electron Beam Melting. *Journal of Materials Engineering and Performance*, 22(12), 3872–3883. https://doi.org/10.1007/s11665-013-0658-0

Rocha, R. C., Galdino, A. G. de S., Silva, S. N. da, & Machado, M. L. P. (2018). Surface, microstructural, and adhesion strength investigations of a bioactive hydroxyapatite-titanium oxide ceramic coating applied to Ti-6Al-4V alloys by plasma thermal spraying. *Materials Research*, 21(4). https://doi.org/10.1590/1980-5373-mr-2017-1144

Sidane, D., Chicot, D., Yala, S., Ziani, S., Khireddine, H., Iost, A., & Decoopman, X. (2015). Study of the mechanical behavior and corrosion resistance of hydroxyapatite sol–gel thin coatings on 316 L stainless steel pre-coated with titania film. T*hin Solid Films*, 593, 71–80. https://doi.org/10.1016/j.tsf.2015.09.037

Silva Junior, W. C., Souza, C. M. P. D. S., Bortoli, F. D. S., Frajuca, C., & Souza, R. C. (2021). Obtaining the predicted number of cycles of femoral prosthesis manufactured with ASTM F138 and ASTM F75 aloys, applying the method of finite element. *Journal of Physics. Conference Series*, 1730 (1)(012026).

Souza, C. M. P. de, Santos, R. G., Souza, R. C., Militão, V. A., Silva, I. G., Seriacopi, V., & Junior, W. C. da S. (2022). Data analyses of fatigue tests by extensometry in hip prosthesis of the Co-28Cr-6Mo alloy. *Research, Society and Development*, 11(4), e52011427854–e52011427854. https://doi.org/10.33448/rsd-v11i4.27854

Wang, D. G., Chen, C. Z., Ma, Q. S., Jin, Q. P., & Li, H. C. (2013). A study on in vitro and in vivo bioactivity of HA/45S5 composite films by pulsed laser deposition. *Applied Surface Science*, 270, 667–674. https://doi.org/10.1016/j.apsusc.2013.01.117